Structure of Micelle-Associated Alamethicin from ^{1}H NMR. Evidence for Conformational Heterogeneity in a Voltage-Gated Peptide†

J. Craig Franklin, Jeffrey F. Ellena, Sajith Jayasinghe, Laurie P. Kelsh, and David S. Cafiso*

Department of Chemistry and Biophysics Program at the University of Virginia, Charlottesville, Virginia 22901

Received October 14, 1993; Revised Manuscript Received January 28, 1994®

ABSTRACT: Alamethicin is a 20 amino acid peptide that produces a voltage-dependent conductance in membranes. To understand the mechanism by which this peptide becomes voltage-gated, the structure of alamethicin bound to micelles was examined using high-resolution ^{1}H nuclear magnetic resonance (NMR). Two-dimensional correlation and nuclear Overhauser effect spectroscopy (NOESY) were carried out on alamethicin incorporated into perdeuterated sodium dodecyl sulfate (SDS) micelles, and the ^{1}H NMR spectrum of the peptide in micelles was assigned. The intensities of the HN–HN$_{(i,i+1)}$, Hα–HN$_{(i,i+1)}$, Hα–NH$_{(i,i+3)}$, Hα–H$\beta_{(i,i+3)}$, and Hα–NH$_{(i,i+4)}$ cross peaks in the NOESY spectrum suggest that the N-terminal half of the peptide is predominantly α-helical, while the C-terminal half has a less regular or more flexible structure. The exposure of micelle bound alamethicin to the aqueous solution was determined by examining the effect of aqueous paramagnetic reagents on the line widths of the peptide protons. These measurements suggest that alamethicin is buried in the micelle. A set of restraints consisting of 175 distances (derived from NOESY spectra), five dihedral angles, and two hydrogen bond distances were used in a simulated annealing procedure that yielded structures for micelle associated alamethicin. The structures that were generated with simulated annealing were largely helical from residues 4–9 and 12–16. A limited number of structural forms were obtained. The main difference among forms involved the backbone conformations of MeA10, Gly11, and Leu12 and resulted in structures that were straight or had different amounts of bend. The structural forms could be easily interconverted by rotation of the ϕ and ψ angles of residues 10–12. The rotational freedom at or near MeA10 may be a result of Pro14, which would be the normal hydrogen-bonding position for the peptide carbonyl of MeA10. These results suggest that conformation rearrangements at or near MeA10 may play a role in the voltage-gating of alamethicin.

The role of membrane electrostatics in controlling the activity of membrane proteins, such as the sodium and potassium channels of nerve cells, is well documented. However, the structures of these channels and the molecular mechanisms that lead to voltage-gating remain largely uncharacterized. In part, this is a result of the difficulty associated with structural studies on large intrinsic membrane proteins. As a result, smaller peptide channels such as alamethicin are being investigated because they provide ideal model systems for voltage-gating phenomena. In addition, alamethicin belongs to a larger family of membrane active peptides that form channels in bilayers. Some of these peptides, such as the magainins and defensins, have immunological roles (Bernheimer & Rudy, 1986; Lehrer *et al.*, 1993; Zasloff, 1987), and molecular information on alamethicin could provide insight into the mechanisms by which the magainins and defensins act. At a more fundamental level, studies on alamethicin facilitate the characterization of protein–membrane electrostatic interactions and the energetics of protein association with lipid bilayers, information that has an impact on our understanding of other important processes such as the interaction of signal sequences with membranes.

Alamethicin is a small 20 amino acid peptide from the fungus *Trichoderma veride* that produces a voltage-dependent conductance in bilayer systems. It contains the unusual amino acid α-methylalanine (MeA, or α-aminoisobutryic acid, Aib),[1] which is generally found in α- or 3_{10}-helical structures (Karle & Balaram, 1990). Also present are two proline residues at positions 2 and 14. Alamethicin is a relatively hydrophobic peptide that would form a weakly amphipathic helix and a popular model for the channel structure is an aggregate of helical monomers. A number of models have been proposed to account for the voltage dependence of alamethicin that are fundamentally quite different. In the crystal structure alamethicin is helical with a bend near Pro14, a structure that inspired the model shown in Figure 1A (Fox & Richards, 1982). In this model, the peptide is in an aggregated form and each monomer undergoes a voltage-dependent conformational rearrangement, enabling the aggregate to insert across the membrane to form a transmembrane pore. Based in part on evidence for β-structure in alamethicin, a similar type of mechanism was proposed in which a portion of alamethicin was aggregated to form a β-barrel (Hall *et al.*, 1984). In this model the N-terminus, which is located on the same side of the membrane as the C-terminus in the closed state, crosses the membrane in response to a potential. Several models for the voltage-gating are proposed that involve quite different mechanisms. In the model shown in Figure 1B, the closed alamethicin channel is formed from an aggregate of antiparallel alamethicin monomers. Transmembrane voltages open the channel by producing a flip-flop of monomers so that

† This work was supported by a grant from the National Institutes of Health (GM-35215 to D.S.C.).

® Abstract published in *Advance ACS Abstracts,* March 1, 1994.

[1] Abbreviations: COSY, 2D correlated spectroscopy; CVFF, consistent valence force field; DQF-COSY, double-quantum filtered COSY; DTPA^{2-}, diethylenetriaminepentaacetic acid; EPR, electron paramagnetic resonance; MeA, α-methylalanine; NMR, nuclear magnetic resonance; NOE, nuclear Overhauser effect; NOESY, 2D nuclear Overhauser effect spectroscopy; RMSD, root mean square distance; ROESY, 2D rotating frame Overhauser enhancement spectroscopy; SDS, sodium dodecyl sulfate; TOCSY, total correlation spectroscopy.

0006-2960/94/0433-4036$04.50/0 © 1994 American Chemical Society

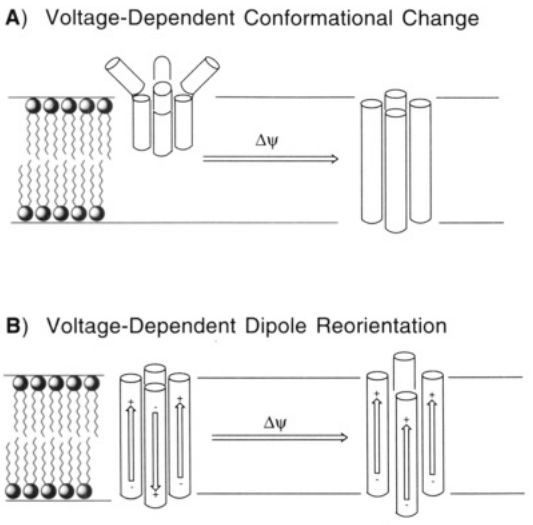

FIGURE 1: Models for the gating of alamethicin: (A) a model involving a voltage-dependent conformational change in alamethicin that leads to the transmembrane insertion of an alamethicin aggregate [see Fox and Richards (1992)]; (B) a model that involves the voltage-dependent reorientation of the alamethicin helix, leading to electrostatic repulsion in the aggregate and an opening of the channel [see Boheim et al (1983)].

helices in the aggregate are arranged with their dipole moments aligned in a parallel (high-energy) configuration (Boheim *et al.*, 1983). This and other models do not require any flexibility in the backbone of the alamethicin monomer. While several models for the gating of alamethicin appear to be less viable than others based on the available experimental evidence, the mechanism by which this peptide becomes voltage-gated has not been identified.

A knowledge of the structure and dynamics of alamethicin, even in the absence of membrane fields, is valuable for understanding its channel activity, and spectroscopic tools such as NMR can provide this information. NMR studies have been undertaken on alamethicin in solution, but because of its limited solubility in water, these studies have been carried out in nonaqueous solvents (Banerjee *et al.*, 1983; Esposito *et al.*, 1987; Chandrasekhar *et al.*, 1988; Kelsh et al., 1992; Yee & O'Neil, 1992). Almost all of these reports conclude that alamethicin is helical in its N-terminal domain; however, β-sheet (Banerjee *et al.*, 1983), α-helix (Esposito *et al.*, 1987), or multiple conformations (Yee & O'Neil, 1992) have been reported for the C-terminus of alamethicin. In methanol, the rotational correlation time of relatively small peptides such as alamethicin is not favorable for obtaining longer range NOEs such as $H\alpha$–$NH_{(i,i+3)}$ and $H\alpha$–$NH_{(i,i+4)}$; as a result, NMR structures based on NOESY data depend on short-range distance restraints (Esposito *et al.*, 1987). In one case, the ROESY experiment (Bothner-By *et al.*, 1984; Bax & Davis, 1985a) was used to overcome this problem (Yee & O'Neil, 1992). NMR studies of alamethicin in phospholipid bilayers have focused on the effect of alamethicin on the bilayer lipids and the membrane-bound location of the peptide (Banerjee *et al.*, 1985, and references therein).

The structure of alamethicin in a micelle environment has not previously been reported. Micelles, while clearly not membranes, provide a heterogeneous environment that is closer to that of a bilayer than bulk solvents such as methanol. Because of the slower rotational correlation time for the peptide in micelles, cross-relaxation should be more efficient, in principle leading to a better defined structure. In the present work, high-resolution ^1H NMR data for alamethicin in SDS micelles is reported along with structures generated by simulated annealing (Nilges *et al.*, 1988) using restraints derived from this data. The data that are presented indicate that the N-terminal domain of alamethicin in micelles is helical, similar to the conformation in nonaqueous solution. However, several distinct low-energy structures having straight and bent configurations are identified in the present analysis. Surprisingly, these conformers appear to result from rotations about just six backbone bonds in the alamethicin structure. These structural forms are discussed in terms of the mechanisms for voltage-gating of this peptide.

EXPERIMENTAL PROCEDURES

Materials. Sodium dodecyl sulfate and D_2O were obtained from Cambridge Isotopes (Woburn, MA). Alamethicin was obtained from Sigma Chemical Co. (St. Louis, MO) and was purified using high-performance liquid chromatography (HPLC) on a reverse-phase C18 column (Vydac, 201TP101) using isocratic 60% acetonitrile/40% water, each containing 0.1% trifluoroacetic acid. The first major fraction eluting at 17 min contained Ala at position 6 and Gln at position 18 (Kelsh *et al.*, 1992). The sequence of this fraction is Ac-MeA-Pro-MeA-Ala-MeA-Ala-Gln-MeA-Val-MeA-Gly-Leu-MeA-Pro-Val-MeA-MeA-Glu-Gln-Phol, and this was the fraction used in this study. Spin-labeled alamethicin was prepared by carbodiimide coupling of the proxyl acid spin label to the C-terminal phenylalaninol residue as described previously (Archer *et al.*, 1991). The chelate gadolinium diethylenetriaminepentaacetic acid (Gd-$DTPA^{2-}$) was obtained from Berlex (Wayne, NJ). Samples for NMR spectroscopy were prepared by codissolving sodium dodecyl sulfate-d_{25} (200 mg) and alamethicin (12.9 mg) in 5 mL of benzene/MeOH, 95:5, and methanol was added until the solution cleared. The mixture was then frozen, lyophilized, and rehydrated with the appropriate buffer to form a solution 5 mM in alamethicin and 500 mM in SDS. No particulates or light scattering could be detected following the addition of buffer. For the DQF-COSY and TOCSY experiments, the buffer was H_2O/D_2O, 9:1, containing 10 mM sodium phosphate, pH 7.0. For the NOESY experiments, the same buffer was used except that the pH was adjusted to 4.0 so that exchange of amide protons with H_2O and loss of amide intensity due to solvent saturation was minimized.

NMR Spectroscopy. NMR spectra were obtained using General Electric Omega 500 and Varian Unity Plus 500 spectrometers operating at a frequencies of 500.13 and 499.84 MHz, respectively. All spectra were recorded at a temperature of 25 °C, chemical shifts were referenced to internal H_2O at 4.75 ppm, and the sweep width was 5 kHz. The H_2O resonance was suppressed by CW irradiation for 1.5 s at the beginning of all experiments. The programs Felix (Biosym Technologies, San Diego, CA) and NMR1 (New Methods Research Inc., East Syracuse, NY) running on an IBM RS6000 340 or a Silicon Graphics Indigo R4000 XZ were used to process the NMR data. The DQF-COSY spectrum (Piantini *et al.*, 1982; Rance *et al.*, 1983) contained 824 and 4096 complex points in the t_1 and t_2 dimensions, respectively. Initial processing included apodization in both dimensions with a sine squared function shifted by 30° and zero filling to 2048 points in the t_1 dimension. The same DQF-COSY spectrum was used to obtain coupling constants except that a 1-Hz exponential was used as the apodization function. Slices were then taken through the appropriate regions of cross peaks, summed, inverse Fourier transformed, zero filled to 8192 points, and Fourier transformed. All $J_{\alpha H\text{–}NH}$ values except those for Gly11 were obtained by fitting the αH–NH antiphase doublets to

two Lorentzians. The Gly11 $J_{\alpha H-NH}$ values were obtained by measuring the passive splittings on the α1H–α2H cross peak (a 30°-shifted sine squared apodization was used in this case). The TOCSY experiment (Braunschweiler & Ernst, 1983; Bax & Davis, 1985b) was carried out using a 100-ms clean (Griesinger *et al.*, 1988) MLEV-17 spin lock, where *Z* filters preceded and followed the spin lock (Rance, 1987). NOESY spectra (Jeener *et al.*, 1979; Macura & Ernst, 1980) were obtained at mixing times of 50, 100, 150, and 250 ms. A composite 180° pulse (90_x, 180_y, 90_x) in the middle of the mixing period improved solvent suppression, and 5-ms homospoil pulses were used at the beginning of the mixing period and after the composite 180° pulse (Blake *et al.*, 1991). The number of complex points collected for TOCSY and NOESY spectra was 512 and 2048 in the t_1 and t_2 dimensions, respectively; the spectra were apodized with a 3-Hz exponential in t_1 and a 90°-shifted sine squared bell in t_2, t_1 was zero-filled to 1024 points.

Analysis of NMR Data and Molecular Structure Determination. Resonance assignments were made following a general procedure described previously (Wüthrich, 1986). In the first step of this process, spin systems were identified using DQF-COSY and TOCSY experiments, followed by sequential assignments of the residues using NOESY NH–NH cross peaks. NOESY cross peak volumes were converted to interproton distances by the method of Baleja *et al.* (1990). Distances were sorted into three categories having upper and lower bounds of 1.8–2.7, 2.7–3.3, and 3.3–5.0 Å. Coupling constants were converted to dihedral angle restraints using $J_{NH\alpha} \leq 5.5$ Hz, $-40° < \phi < -90°$; 8.5 Hz $< J_{NH\alpha} <$ 10 Hz, $-160° < \phi < -80°$ (Karplus, 1959; Pardi *et al.*, 1984; Akke *et al.*, 1992).

The molecular modeling of alamethicin was carried out using InsightII (version 2.2), Discover (version 2.9), and NMRchitect (version 2.0) (Biosym Technologies, San Diego, CA) running on a Silicon Graphics Indigo R4000 XZ workstation and employing the Biosym CVFF force field. Three stages of distance geometry (bound smoothing, embedding, and optimization) were used to generate 10 structures (Crippen & Havel, 1978; Havel & Wüthrich, 1985; Havel, 1990). Error violations greater than 0.3 Å for all structures were compiled and examined. Most of the errors were the result of incorrect integration of cross peaks due to spectral overlap or baseline distortions. In cases where it was not possible to deconvolute the peaks or correct for spectral overlap, the distances were discarded or the upper and lower limits were expanded to reflect the uncertainty in the distance. Sixty distances were eliminated from the list of restraints because it was not possible to deconvolute the overlap.

The simulated annealing (Nilges *et al.*, 1988) protocol used was similar to one implemented in the NMRchitect software and is shown in Table 1. The restraints included 175 NOE distances, five dihedral angles, and two hydrogen bonds. The cutoff distance for nonbond interactions was 10 Å. The dynamics integration time step was 0.5 ps, and the force constants for NOE distance and dihedral angle terms were 50 and 150 kcal mol^{-1}, respectively. One of the distance geometry structures was used as the starting structure, and 120 structures were generated. Following annealing, the full CVFF force field and the NMR restraints were used to energy minimize the structures to a final derivative of 0.001 kcal mol^{-1} Å^{-1}. The dielectric constant was 4, and the cutoff for nonbond interactions was 20 Å.

Other Procedures. To determine the exposure of alamethicin in SDS to the aqueous solution, the effect of a water soluble relaxation reagent on the ^{1}H alamethicin resonances in SDS was examined. In these experiments, gadolinium diethylenetriaminepentaacetic acid (Gd-DTPA^{2-}) was added to the alamethicin–SDS mixture described above so that the final chelate concentration was 44 mM. The effect of the Gd-DTPA^{2-} was measured by comparing the intensities of the TOCSY cross peaks in the presence and absence of Gd-DTPA^{2-} using a procedure similar to that described previously (Esposito *et al.*, 1992).

Amide exchange rates for alamethicin in SDS were measured by preparing the alamethicin SDS sample as described above, except that deuterium oxide rather than water was added to the lyophilized SDS alamethicin mixture (pD 3.5, uncorrected). The first one-dimensional spectra was recorded 30 min after the addition of deuterium oxide. TOCSY experiments (128 complex points in t_1, 1024 complex points in t_2, 16 scans per t_1, mixing time 100 ms) were recorded after 1.2, 2.25, 4.0, 6.0, 8.0, 12.0, 19.0, 24.5, 30.0, and 44 h. Cross peaks involving amide protons were integrated, and the intensity was fitted to a single-exponential curve. At least two cross peaks per amide proton were used to describe the exchange rate.

EPR spectra for spin-labeled alamethicin samples in methanol and SDS were recorded on a Brüker ESP 300 series X-band spectrometer using an incident microwave power of 20 mW and a modulation amplitude of 2g p–p. The spectra were recorded from samples in a 100-μL quartz flat cell in a cavity resonator at a nitroxide concentration of approximately 50 μM.

Table 1: Simulated Annealing Protocol

procedure	force[a]	% of final value[b]	K	duration (ps)
randomize coordinates, energy minimize	covalent	0.0001		
	nonbond	0.0001		
	distance	0.0001		
	dihedral	0.0001		
	chiral	0.0001		
dynamics	covalent	0.0001 → 0.02		6
	nonbond	0.0001 → 0.1		
	distance	0.0001 → 0.1		
	dihedral	0.0001 → 0.1		
	chiral	0.0001 → 0.1		
dynamics	covalent	0.02 → 15	1000	5
	nonbond	0.1 → 1		
	distance	0.1 → 50		
	dihedral	0.1 → 50		
	chiral	0.1 → 15		
dynamics	covalent	15 → 100	1000	5
	nonbond	0.1 → 1.5		
	chiral	15 → 100		
dynamics	nonbond	1.5 → 25	650	2
	distance	50 → 100		
	dihedral	50 → 100		
dynamics			475	2
dynamics			385	2
dynamics			340	2
dynamics			300	4

[a] Only diagonal forcefield terms and no charges were included. Forces are listed only if they were different than in the preceding step. [b] Percent of final values are listed only if they were different than in the preceding step. If two numbers are separated by an arrow, they are the initial and final values during the step.

RESULTS

SDS-Bound Alamethicin Is Monomeric and Yields a High-Resolution ^{1}H Spectrum. There are a number of indications that alamethicin is completely micelle associated, uniformly dispersed, and monomeric in the SDS sample. Alamethicin

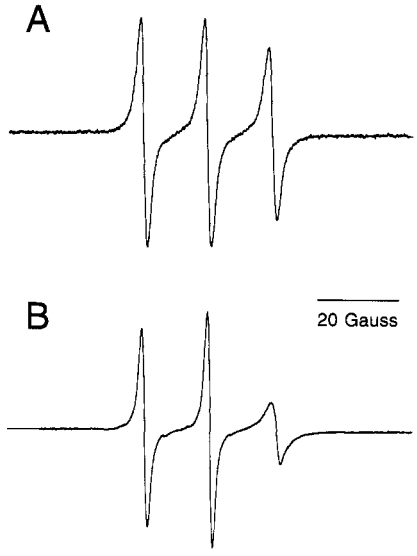

FIGURE 2: spectra of a proxyl nitroxide alamethicin derivative in (A) methanol at a concentration of 50 μM and in (B) 500 mM SDS micelles at a concentration of 0.5 mM (the spectrum is identical at a label concentration of 5 mM).

has a large membrane–aqueous partition coefficient, and the limit of alamethicin solubility in water is 20 μM (Archer *et al.*, 1991). The total alamethicin concentration used here greatly exceeds this value, and given the high concentration of SDS used, it is unlikely that any significant level of alamethicin is present in the aqueous phase. Unlike aqueous dispersions, no light scattering from SDS-solubilized alamethicin could be detected. However, as a check on the aggregation state of alamethicin in the SDS preparation, a spin-labeled analogue of alamethicin with a proxyl label on the C-terminus was incorporated into methanol and SDS preparations of alamethicin. This probe is monomeric in methanol (Archer *et al.*, 1991), and the EPR line shape corresponds to an effective probe correlation time of 0.12 ns. Shown in Figure 2 are EPR spectra of the spin-labeled alamethicin analogue in methanol and in SDS solution under the conditions used in the NMR experiments. The spectrum in SDS corresponds to a single component, which would not be expected if alamethicin were partitioning between the aqueous and micelle phases. The line shape in SDS is more anisotropic and broader than in methanol and corresponds to a rotational correlation time near 0.9 ns, consistent with the slower rotational correlation time expected for alamethicin in micelles. Furthermore, there is a linear relationship between signal intensity and peptide concentration in SDS from 5 μm to 5 mM, indicating that the nitroxide line shape is constant over a wide range of concentrations. Changes in the aggregation state of the peptide should dramatically alter the line shapes as a result of changes in the rotational correlation time and collisional spin-exchange. These data indicate that the peptide is monomeric in SDS and that it remains monomeric at least up to 5 mol % in SDS.

The ^{1}H NMR spectra of alamethicin in SDS micelles are well-resolved, and the line widths, although broader than in methanol, provide high-resolution data. This also provides an indication that extensive aggregation of alamethicin is not occurring in these samples. Shown in Figure 3 is a 2D NOESY spectrum for alamethicin in SDS showing dipolar cross-relaxation between protons in the peptide. Figure 3B shows an expansion of the amide proton region clearly revealing dipole–dipole interactions and some of the sequential NOEs between amide protons along the backbone.

Resonance Assignments and a Secondary Structure Analysis from Chemical Shifts. The resonance assignments for alamethicin in methanol were previously reported (Espositio *et al.*, 1987); however, the chemical shifts and the relative positions of resonances found here in SDS differed from those in methanol and required that the spectrum be independently assigned. To identify spin systems and assign the NMR spectrum of alamethicin in SDS, two-dimensional DQF-COSY and TOCSY spectra were recorded. The TOCSY experiment identifies protons within a spin system, while the DQF-COSY spectra provide information on the covalent arrangement of protons within the spin system. Shown in Figure 4 is the region of the TOCSY spectra showing scalar coupling between HN protons and the side chain protons of Ala4, Ala6, Gln7, Val9, Val15, Gln19, and Phol20.

Shown in Table 2 are the chemical shift assignments for alamethicin in SDS. While the average proton chemical shifts in SDS are similar to those for methanol (the average difference between resonances in each environment is 0.02 ppm), there was a standard deviation of 0.13 ppm, and several shifts differed by as much as 0.37 ppm. As expected, the line widths in SDS are larger than those in methanol, which made resolving several of the resonances difficult. A number of resonances that can be uniquely assigned in methanol cannot be uniquely assigned in SDS. The 16 MeA β methyls proved to be particularly difficult to uniquely assign, and, because of spectral overlap, none of the MeA β protons were used in generating interproton distances.

A recent analysis of chemical shift information from proteins of known structure demonstrates that the difference between the Cα proton chemical shift in a protein structure and the shift in a random coil (called the "chemical shift index") correlates well with protein secondary structure (Wishart *et al.*, 1992). A helical structure is indicated by a chemical shift index of –0.1 ppm or less for four or more consecutive residues, while β-sheet structures are indicated by a chemical shift index of +0.1 or larger for at least three consecutive residues. The termination of a stretch of secondary structure is indicated by a change in the sign of the index or a change of the chemical shift indexes to zero for two or more residues. Figure 5 shows a graph of the chemical shift index calculated from the chemical shifts in methanol and SDS. Since a random coil value for the MeA residues is not known and because the validity of this analysis for MeA has not been established, the eight MeA residues in alamethicin are not shown.

The chemical shift index for alamethicin suggests that in both methanol and SDS the first 11 residues are in a helical configuration. The structure of alamethicin in SDS differs slightly from that in methanol, beginning at Gly11. Compared to the SDS structure, the structure in methanol appears to be slightly more helical in this region, and only one position (compared to three for the SDS structure) has a positive chemical shift index. From the chemical shift index of the Gly11 protons, the helix appears to extend through Gly11 in methanol but falls within the values predictive of a random coil in SDS.

Interresidue NOEs, Coupling Constants, and Alamethicin Secondary Structure. The magnitudes and pattern of the interresidue nuclear Overhauser effects can be used to provide a qualitative indication of the secondary structure of proteins (Wüthrich, 1986). Figure 6 shows the interresidue proton NOEs for alamethicin in SDS micelles. The HN–HN$_{(i,i+1)}$, Hα–HN$_{(i,i+3)}$, Hα–H$\beta_{(i,i+3)}$ and Hα–HN$_{(i,i+4)}$ cross peaks due to residues in the N-terminal half of the peptide suggest that it has a helical secondary structure. The presence of Hα–

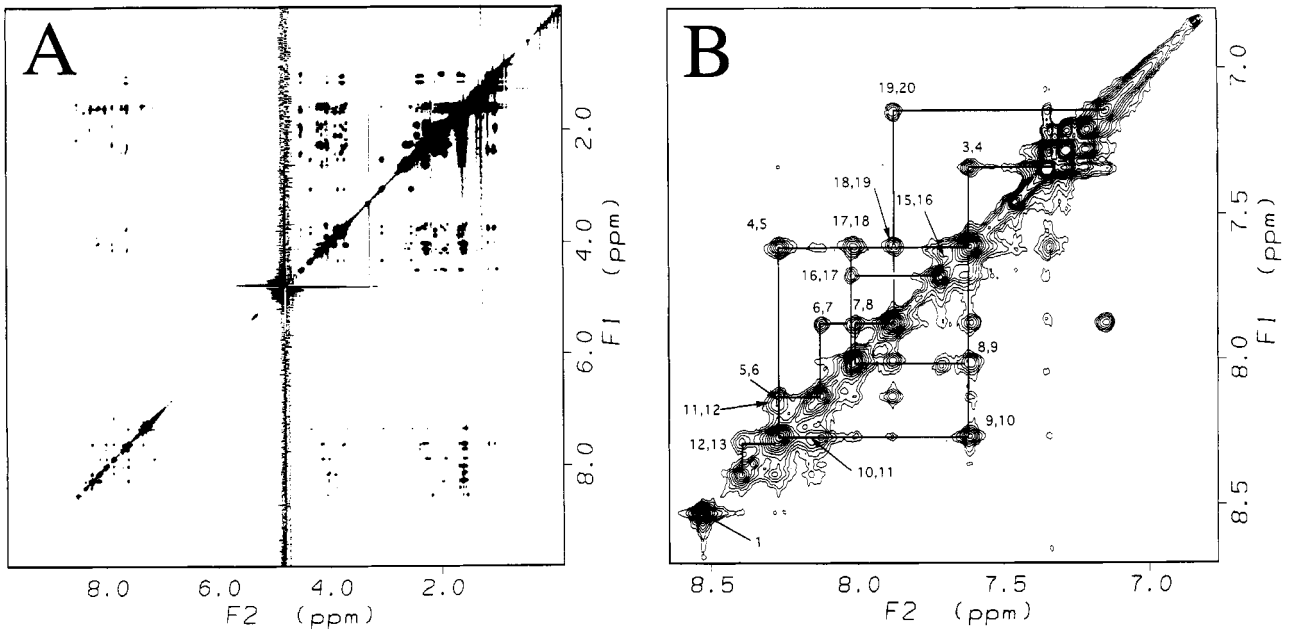

FIGURE 3: (A) 500-MHz ^{1}H–^{1}H NOESY spectrum at a mixing time of 250 ms for 5 mM alamethicin in 500 mM SDS-d_{25} at 25 °C and pH 4.0. This plot consists of 1024 × 2048 complex data points. (B) An expansion of the spectrum shown in panel A for just the amide protons, indicating sequential connectivities (i,i+1) for amide residues.

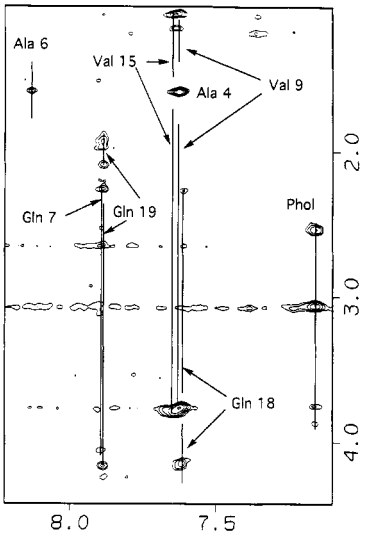

FIGURE 4: Portion of the 500-MHz ^{1}H–^{1}H TOCSY spectrum at 100-ms mixing time for 5 mM alamethicin in 500 mM SDS-d_{25} at 25 °C and pH 7.0. The spectrum allows the identification of spin systems by correlations between amide protons and sidechain α, β, and γ protons.

$HN_{(i,i+4)}$ crosspeaks suggests that the helix is α rather than 3_{10} (Wüthrich, 1986).

Another trend that is apparent in the data shown in Figure 5 is the reduction of long-range distances in the C-terminal region of the peptide. The frequency and amplitude of the NOE cross peaks diminish on the C-terminal side of Gly11, and suggest that the helix ends at this point in the structure. The HN–$HN_{(i,i+1)}$, Hα–$NH_{(i,i+3)}$, and Hα–H$\beta_{(i,i+3)}$ cross peaks on the C-terminal side of Gly11 suggest the beginning of a second helical structure.

The relationship between H_α and H_N scalar coupling and secondary structure has been well characterized (Karplus, 1959; Pardi *et al.*, 1984). Coupling constants for those residues in alamethicin containing both Hα and HN protons have been measured and are listed in Table 3. Coupling constants less than 5.5 Hz indicate ϕ angles from –90° to –40° and are consistent with a helical structure. All of the residues beginning at the N-terminus through Gly11 have coupling constants (with the exception of Val9) that correlate with a helix. Given that MeA residues are usually associated with helices, the entire N-terminal domain is likely to be helical.

Table 2: Proton Chemical Shift Assignments for Alamethicin in SDS Micelles[a]

	δ (ppm)				
residue	NH	α	β	γ	δ
MeA1	8.48		1.49		
n			1.58		
Pro2		4.16	2.21	2.12	4.00
			1.95	1.83	3.64
MeA3	7.29				
Ala4	7.56	4.11	1.53		
MeA5	8.22		1.63		
Ala6	8.08	3.97	1.59		
Gln7	7.83	3.98	2.23	2.57	
			2.19	2.48	
MeA8	7.96		1.64		
Val9	7.56	3.69	2.28	1.11	
				1.00	
MeA10	8.21		1.51		
Gly11	8.11	3.99			
		3.87			
Leu12	8.23	4.45	1.95	1.92	0.98
			1.63		0.95
MeA13	8.35	1.635			
Pro14	4.46		2.38	2.05	3.85
			1.88		3.75
Val15	7.58	3.73	2.35	1.10	
				1.00	
MeA16	7.66				
MeA17	7.97				
Gln18	7.56	4.075	2.22	2.59	
			2.20	2.53	
Gln19	7.82	4.08	1.87	2.02	
			1.89		
Phol20	7.10	4.29	β 3.00	ortho 7.29	
			β 2.48	meta 7.24	
			β′ 3.80	para 7.17	
			β′ 3.68		

[a] Assignments for alamethicin in SDS micelles are referenced to water at 4.8 ppm and were obtained from the DQF–COSY and TOCSY spectra at pH 7, 25 °C, in 10 mM $NaHPO_4$ with 10% D_2O.

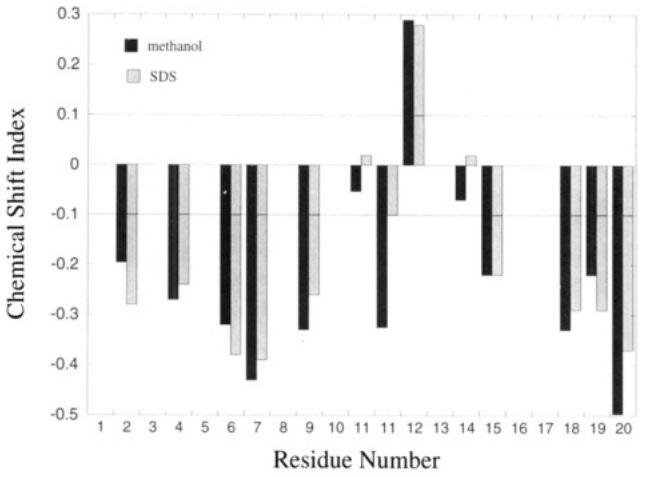

FIGURE 5: Chemical shift index as a function of residue position for alamethicin in methanol (Esposito *et al.*, 1987) and SDS (Table 2). This index is the difference between the Ca proton chemical shift of non-MeA residues of alamethicin and the chemical shifts that those residues have in a random coil configuration (Wishart *et al.*, 1992).

$J_{H\alpha-HN}$ values for residues 12–20 are consistent with nonregular structure and/or multiple conformations.

Alamethicin Is Uniformly Buried into SDS Micelles. To determine the exposure of alamethicin to the aqueous solution when bound to SDS micelles, the paramagnetic chelate Gd-DTPA^{2-} was used to produce selective broadening of the residues in the aqueous phase. The Gd-DTPA^{2-} concentration used here produces greater spin–spin relaxation in the head group region of the SDS micelles compared to that in the acyl chains by a factor of 2.5, and is expected to produce greater relaxation for alamethicin residues exposed to the aqueous solution. Using the procedure described above (see Experimental Procedures), Gd-DTPA^{2-} reduced the intensities of the alamethicin COSY cross peaks on average by a factor of about 4. Comparison of the NH–Cα cross peaks along the backbone indicated that no region of the peptide appeared to be selectively relaxed by or protected from this paramagnetic reagent. Thus, specific domains of alamethicin do not appear to be selectively protected by the SDS from the aqueous solution.

Several studies (Henry & Sykes, 1990; O'Neil & Sykes, 1988) have characterized the amide exchange rates of the membrane spanning M13 coat protein solubilized in SDS. Protons in hydrophobic membrane-spanning regions have exchange rates much slower than aqueous accessible regions. For alamethicin in SDS, the exchange rates, with the exception of MeA1 and Phol20, are between 1.5 and 8.7 $\times$ 10^{-4} s^{-1} at pH 4. The only residue having an exchange rate consistent with the aqueous portion of the M13 coat protein is MeA1. Slow exchange rates could be the result of a stable, secondary structure and/or an intramicellar location for alamethicin. Taken together with the paramagnetic effects described above, the data are consistent with a buried location for alamethicin within the micelle interior.

NMR Data and Simulated Annealing Yield Alamethicin Structures. Distance geometry was used to check for misassignment of NOE cross peaks and improper integration due to spectral overlap or baseline distortions. NOE interactions, particularly $H\alpha_{(i)}$–$H\beta_{(i+3)}$ and $H\alpha_{(i)}$–$HN_{(i+4)}$ and $J_{H\alpha-HN}$ for residues 4–9 strongly suggest this region is a right-handed α-helix (Wüthrich, 1986; Gippert *et al.*, 1990). Therefore, the following hydrogen bonds must be present: Ala4 O–MeA8 NH and MeA5 O–Val9 NH. These were added to the restraint list; the lower and upper distance limits were set to 1.8 and 2.7 Å, respectively. The following restraint set was used during the simulated annealing and subsequent energy minimization: 175 NOE distance (72 intraresidue and 103 interresidue), five dihedral, and two hydrogen bond restraints. When hydrogen bonds were not included in the restraint set, occasional low energy structures that had a left-handed helical structure in the N-terminal six or seven residues were observed. These structures were eliminated by inclusion of the hydrogen bonds.

Shown in Figure 7A are the 30 lowest energy structures obtained from 120 simulated annealing runs that have their backbone atoms from residues 4 to 9 superimposed. With the exception of the first few residues on the N-terminus, the structures appear to align very well over the N-terminal half of the molecule. The structures are clearly different as evidenced by their poor alignment in the C-terminal domain. Alignment of residues 12–16 is good when the backbone atoms of these residues are superimposed (Figure 7B). Alignment of residues 10 and 11 are poor regardless of which residues are superimposed. A closer examination of the structures shows that a limited number of conformeric forms of alamethicin have been generated by the simulated annealing. The structures have been grouped on the basis of similarity in Figure 8 and can be divided into eight sets based on their conformations from residues 4–16. The backbone atoms of residues 4–16 in each of Figure 8, panels A–C, have been superimposed, and it is clear that the structures within each group are very similar. There are eight structures in each of Figure 8A–C; these structures, between residues 4 and 16, can be characterized as straight (I), highly bent (II), and slightly bent (III), respectively. The backbone atoms of residues 4–9 of the six structures in Figure 8D have been superimposed. Two of the structures in Figure 8D are very similar between residues 4 and 16; however, the others are dissimilar. Also, all the residue 4–16 conformations in Figure 8D are dissimilar to those in Figure 8A–C. In summary, Figure 8 panels A–C consist of one structural form each, and there are five forms in Figure 8D.

Upon consideration of all 30 structures (Figure 7A), one finds that the conformation of residues 1–3 and 17–20 is variable. Also, all structures contain a right-handed α-helix from residues 4 through 9 and an irregular, right-handed helix from residues 12 through 16. The conformations of residues 10 and 11 and to a lesser extent 12 vary among the forms and determine the amount of bend in the center of the structures. Bend angles vary among the forms from very small ($\approx$0°, i.e., form I) to moderate (<45°, i.e., form III) to large (>90°, i.e., form II). The forms in Figure 8D have a variety of bend angles. Energy differences among forms was small compared to the energy variation among structures having the same form. The average energies of the structures in Figure 8 panels A–D was 468 $\pm$ 25, 485 $\pm$ 16, 463 $\pm$ 24, and 490 $\pm$ 15 kcal/mol, respectively.

To more quantitatively evaluate the differences among these structures, the average RMSDs resulting from pairwise alignment of four residue fragments along these structures were compared, and the results are shown in Figure 9. When the entire set of structures is compared (Figure 9A), the differences among these structures is maximal in the middle of the structure and at the ends of the peptide. Two minima in the RMSD values appear in the middle of the N-terminal and C-terminal halves of the peptide. When variation within the first three structural forms (I, II, III) is compared, the maximum in the middle of the structure is no longer seen, while relatively high variation among the structures at each

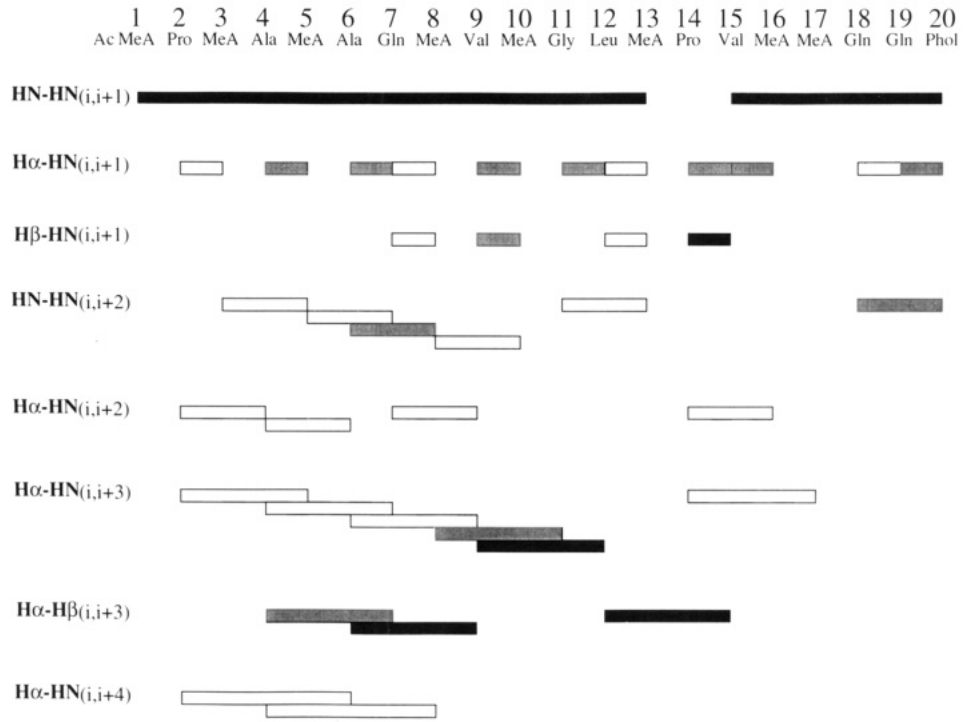

FIGURE 6: Summary of the sequential and short-range NOEs observed for the alamethicin sample in SDS. The NOEs were obtained from the NOESY cross peaks by integrating them and dividing them into three categories: strong (solid bar), medium (shaded bar), and weak (open bar).

Table 3: Intraresidue Scalar Coupling[a]

position	coupling constant (Hz)
Ala4	4.8
Ala6	5.0
Gln7	4.9
Val9	6.7
Gly11:α1	4.0
Gly11:α2	5.2
Leu12	8.4
Val15	6.3
Gln18	7.5
Gln19	8.1
Phol20	9.5

[a] Coupling constants less than 5.5 Hz indicate dihedral angles for the H–N–C–H atoms from –90° to –40° and are consistent with a helical structure. A wide range of dihedral angles are consistent with coupling constants between 5.5 and 8.5 Hz: for these values there is no strong correlation with a specific secondary structure.

end is still present (Figure 9B). A RMSD maximum in the center of the molecule is observed when the structures in Figure 8D are compared. The RMSD dependence on position is consistent with the difference among structural forms arising from conformational variability in the center of the peptide. This was further tested by attempting to convert one form to another by variation of ϕ and ψ dihedral angles near the peptide center.

Average structures for forms I, II, and III were obtained by calculating the average set of atomic positions within each group and energy minimizing the resulting structure. Figure 10 shows residues 4–16 of these average forms. In Form I, the (ϕ, ψ) angles for MeA10 and Gly11 are (–148, 63) and (–169, –46), respectively. By rotation of the ϕ angle of MeA10 for structure II from 52 to –148°, structure IV is obtained. By rotation of the (ϕ, ψ) angles of MeA10 and Gly11 for structure III from (–58, 8) and (67, 29) to the form I values, the structure labeled V is obtained. Structures IV and V closely resemble the straight structure labeled I, indicating that the difference between I and IV arises largely from rotation

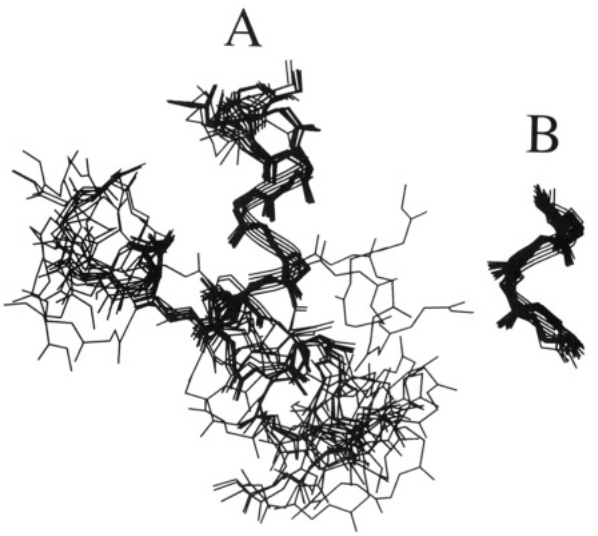

FIGURE 7: (A) The 30 lowest energy configurations obtained out of 120 simulated annealing runs. The backbone atoms of residues 4–9 of 29 structures have been superimposed on the lowest energy structure; only backbone atoms are shown. The ribbon traces the backbone of residues 4–9 of the lowest energy structure with the N-terminus at the top of the figure. In panel B the backbone atoms of residues 12–16 of 29 structures have been superimposed on the lowest energy structure; only backbone atoms are shown. The ribbon traces the backbone of residues 12–16 of the lowest energy structure.

of MeA10 ϕ and the difference between I and V arises from rotations of ϕ and ψ of MeA10 and Gly11. Conversions of the other structural forms (Figure 8D) to form I can be achieved by similar dihedral angle rotations involving MeA10, Gly11, and/or Leu12 (Table 4).

DISCUSSION

The structure of alamethicin has not previously been examined using ^{1}H NMR in amphiphilic environments. Micelles provide a heterogeneous amphiphilic environment

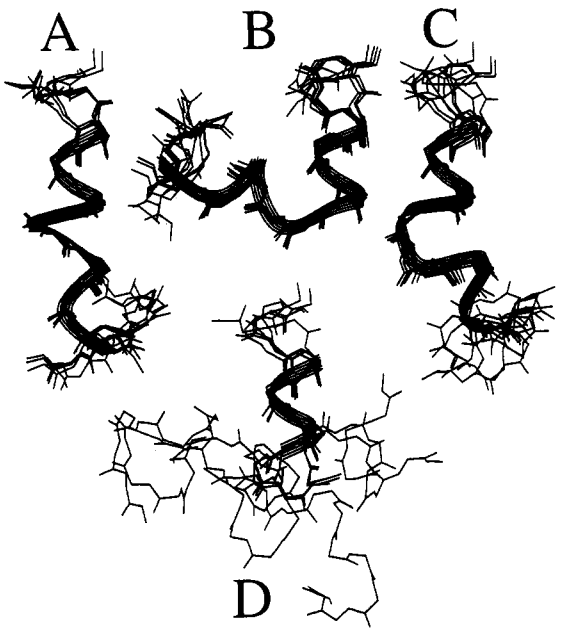

FIGURE 8: Structures in Figure 7 have been put into groups based on structural similarity. A, B, and C each contain eight structures; residues 4–16 of seven structures have been superimposed on the lowest energy structure of the group. The ribbons trace the backbone of residues 4–16 of the lowest energy structure of the group. D contains six structures; residues 4–9 of five structures have been superimposed on the lowest energy structure of the group. The ribbon traces residues 4–9 of the lowest energy structure. Only backbone atoms are shown.

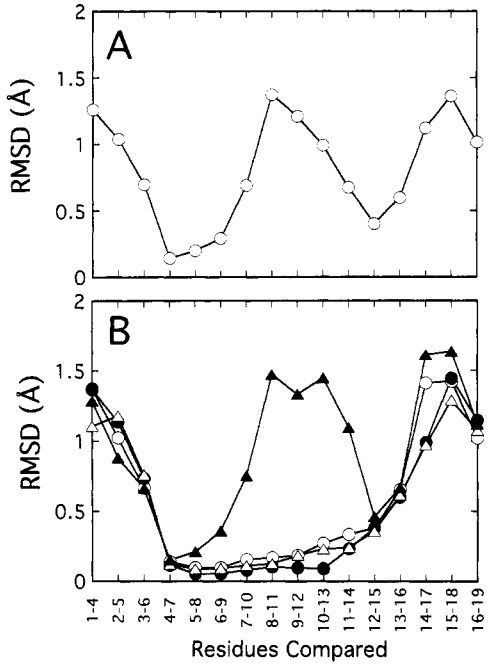

FIGURE 9: (A) Backbone RMSD values in (Å) for the alignment of four amino acid segments for the set of structures seen in Figure 7A. The high RMSD values indicate regions where there is significant variability between structures. (B) Backbone RMSD values (Å) are shown for each of the structural groups shown in Figure 8: (●) Figure 8A, (△) Figure 8B, (○) Figure 8C, and (▲) Figure 8D.

with a hydrocarbon–aqueous interface and are a better approximation to a bilayer phase than solutions. Because of their small size, micelles undergo relatively rapid isotropic motion, yielding a high-resolution spectrum for peptides that are dissolved in their interior. In addition, the motion of the peptide is slower than it would be in solution, making nuclear Overhauser effects more efficient. Unfortunately, the slower motion of the micelle-bound peptide also results in broader

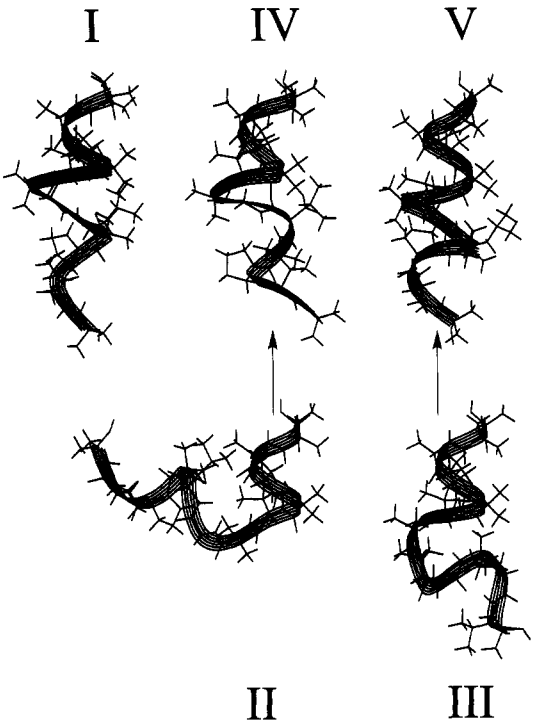

FIGURE 10: Structures labeled I, II, and III are averaged structures obtained from the structures in Figure 8, panels A, B, and C, respectively (see text). Structure IV is obtained by rotation of the ϕ angle of MeA10 in structure II from 52 to −148°. Structure V is obtained by rotation of the (ϕ,ψ) angles of MeA10 and Gly11 in structure III from (−58, −8°) and (67, 29°) to (−148, 63°) and (−169, −46°).

Table 4: Interconversion of Structural Forms[a]

form	residue	ϕ	ψ
I	MeA10	−148	63
	Gly11	−169	−47
	Leu12	−146	−37
II	MeA10	52	
III	MeA10	−58	−8
	Gly11	67	29
4	MeA10	86	
	Gly11	79	18
5	MeA10	146	−73
	Leu12	67	
6	MeA10		−82
	Gly11	−25	
	Leu12	−62	
7	MeA10	−59	−3
	Gly11	67	38
8	MeA10	−58	−53
	Gly11	169	42
	Leu12	45	2

[a] All form I (ϕ, ψ) values for MeA10, Gly11, and Leu12 are given. For other forms only ϕ and/or ψ values are given which, when converted to the form I values, yield a structure which strongly resembles the form I structure when residues 4–16 are compared. Forms I, II, and III are shown in Figure 9. Forms 4–8 are shown in Figure 8D.

^{1}H resonances making spectral assignments of overlapping resonances difficult (such as those from the MeA β protons of alamethicin). The analogy between the bilayer and the micelle phase is clearly not perfect. The micelle interface has a different structure than that of the membrane. In addition, while membranes are clearly highly disordered, approximating a liquid hydrocarbon at their center, detergent amphiphiles are uniformly more disordered than bilayers.

The NMR data obtained here provide a consistent picture of the N-terminal region (residues 4–9) of alamethicin. $J_{\alpha NH}$ values, chemical shifts of the α carbon protons, and NOEs all

suggest that this region of the peptide is α-helical. This observation is consistent with previous NMR data on the solution structure of alamethicin which also provides evidence for a helical N-terminal domain (Banerjee & Chan, 1983; Esposito *et al.*, 1987; Kelsh *et al.*, 1992; Yee & O'Neil, 1992). The structure of the C-terminal domain of alamethicin has been more difficult to define in solution and this is the case in SDS as well. Indeed, even in the crystal structure three forms of alamethicin are seen that vary in the structure of the C-terminal domain. Here, the coupling constants in SDS, chemical shift index, and NOEs all provide a strong evidence that the peptide changes near Gly11 and that there is a break in the helix at this point in the sequence. The Gd-DTPA^{2-} and amide exchange experiments described above provide a strong indication that the differences seen between the N- and C-terminal regions of the peptide are not the result of different exposures of the peptide to the solution.

Simulated annealing provides an approach to combine the available NMR data with the results of molecular dynamics and energy minimization (Nilges *et al.*, 1988). The number of restraints per proton used in our analysis averaged about four and was relatively consistent along the length of the structure. Although more restraints would have been desirable, the results allow us to conclude that a limited number of conformations relatively similar in energy are consistent with the NMR data. The surprising result obtained from this analysis is that the different forms can be interconverted by rotation of the ϕ and ψ dihedral angles for MeA10, Gly11, Leu12, or some subset of these angles. As discussed below, rotation about these angles is physically reasonable.

There is currently a great deal of interest in the role of proline residues in the function of membrane proteins. Proline residues are found in the transmembrane helical regions of membrane proteins at a relatively high frequency, and they have been proposed to modulate both the conformation and dynamics of these transmembrane segments (Williams & Deber, 1991). Alamethicin has prolines at positions 2 and 14, and rotation of the helix about Pro14 was proposed as a mechanism of gating (Fox & Richards, 1982). The structures found here do not provide evidence for conformational variability about Pro14; however, they do indicate that Pro14 plays a critical role in determining the behavior of the peptide. As shown above, the structural forms obtained by simulated annealing are quite similar and differ largely in the values for the ϕ and ψ angles of MeA10, Gly11, and Leu12. In an α-helical configuration, the oxygen on MeA10 would normally be hydrogen bonded to position 14, an interaction that cannot occur with proline. In addition, the Gly11 carbonyl oxygen is hydrogen bonded to solvent in the alamethicin crystal structure. The structural forms resulting from rotations of ϕ and ψ angles of MeA10, Gly11, and/or Leu12 may be a direct consequence of Pro14 and the loss of internal hydrogen bonding in this portion of the structure. The dramatic break from the strong helical tendency in the N-terminus that is seen in the coupling constant and NOE data near MeA10 may result from Pro14. It would obviously be interesting to compare the structures obtained from NMR for analogues where substitutions are made at position 14. Bilayer electrical data have been obtained for non-MeA containing analogues of alamethicin where MeA residues have been replaced by Leu. For these peptides, substitution of Ala for Pro14 does not eliminate the voltage-dependent channel activity of the peptide but does result in shorter channel lifetimes and a lower concentration dependence for the conduction (Duclohier *et al.*, 1992).

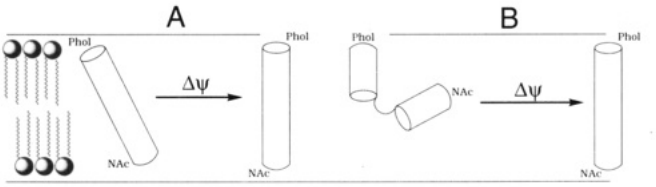

FIGURE 11: Conformational rearrangements that could account for the voltage-gating of alamethicin. In A, the peptide is linear but undergoes a change in its orientation within the membrane. In B, the peptide undergoes a transition from a bent to a linear configuration. These transitions could occur for monomeric alamethicin (leading to subsequent aggregation), or the transitions could take place within aggregates of the alamethicin monomer.

A previous analysis of NOE and relaxation data obtained in methanol led to the conclusion that alamethicin was a relatively rigid rod, which was not rapidly converting between forms such as those depicted in Figure 7 (Kelsh *et al.*, 1992). These data do not necessarily rule out the interconversion of the structural forms found from simulated annealing. If these forms are intercoverting on a slow time scale relative to the tumbling rate of alamethicin in methanol (about 1 ns), they would not contribute to the spectral densities leading to relaxation and would not have been detected. In addition, while methanol is a good solvent for alamethicin, it clearly does not present the peptide with the heterogeneous environment found in SDS. Methanol generally favors the formation of helical structures, and a different behavior resulting from environment is not unexpected.

The mechanism by which alamethicin gates most likely involves a helix dipole. The single negative charge on alamethicin is not required for gating, and the formation or reorientation of a helix dipole within the membrane hydrocarbon is the simplest mechanism that can account for gating. Indeed, recent molecular modeling studies (Galaktionov & Marshall, 1993; Sansom, 1993), in conjunction with a large body of previous work, favor a gating mechanism consisting of voltage-dependent conformational changes and/or reorientation of the peptide with respect to the bilayer. These types of rearrangements are depicted in Figure 11. The observation of both straight and bent alamethicin structures in Figure 7 suggests that the transition shown in Figure 11B is a likely mechanism for the gating of this peptide. In this case, gating occurs because of a change in the net macroscopic dipole moment resulting from the unfolding of the peptide. This rearrangement might occur as a monomer, leading to subsequent aggregation and channel formation; alternatively, the structural change might take place within an aggregated form similar to that depicted in Figure 1A. It should be noted, however, that the available evidence suggests the C-terminus of alamethicin is not exposed to solvent to the extent shown in Figure 1A (Cafiso, 1994). When considering alamethicin structure, one should be aware that even when a voltage is applied across membranes containing alamethicin and ion conduction is occurring, only a small fraction of the alamethicin molecules may be in a conductive state at any given time. Thus it may be very difficult to directly obtain the structure of alamethicin in its active state.

There have not been many reports describing the effect of membrane potentials on the membrane-bound state of alamethicin; however, there is evidence that the peptide helical content increases and β content decreases when trans negative membrane potentials are applied across lipid vesicles (Brumfeld & Miller, 1990). A transition between bent and more linear forms of alamethicin could result in this type of secondary structure change. Currently, efforts in our labo-

ratory are directed at the use of spin-labeled analogues of alamethicin to characterize voltage-driven conformational changes in alamethicin. We are also obtaining additional evidence for the bent form of this peptide in SDS by examining the paramagnetic relaxation effects of spin-labeled alamethicin analogues.

ACKNOWLEDGMENT

We thank Profs. Robert Bryant and Gordon Rule for the use of their Varian NMR spectrometers.

SUPPLEMENTARY MATERIAL AVAILABLE

A full list of the restraints that were obtained from NMR and used in the molecular modeling protocol (6 pages). Ordering information is given on any current masthead page.

REFERENCES

Akke, M., Drakenberg, T., & Chazin, W. (1992) *Biochemistry 31*, 1011–1020.
Archer, S. J., Ellena, J. F., & Cafiso, D. S. (1991) *Biophys. J. 60*, 389–398.
Blake, P. R., Park, J.-B., Bryant, F. O., Aono, S., Magnuson, J. K., Eccleston, E., Howard, J. B., Summers, M. F., & Adams, M. W. W. (1991) *Biochemistry 30*, 10885–10895.
Braunschweiler, L., & Ernst, R. R. (1983) *J. Magn. Reson. 53*, 521–528.
Baleja, J., Moult, J., & Sykes, B. (1990) *J. Magn. Reson. 87*, 375–384.
Banerjee, U., Tsui, F. P., Balaasubramanian, T. N., Marshall, G. R., & Chan, S. I. (1983) *J. Mol. Biol. 165*, 757–775.
Banerjee, U., Zidovetzki, R., Birge, R. R., & Chan, S. I. (1985) *Biochemistry 24*, 7621–7627.
Bax, A., & Davis, D. G. (1985a) *J. Magn. Reson. 63*, 207–213.
Bax, A., & Davis, D. G. (1985b) *J. Magn. Reson. 65*, 355–360.
Bernheimer, A. W., & Rudy, B. (1986) *Biochim. Biophys. Acta 864*, 123–141.
Boheim, G., Hanke, W., & Jung, G. (1983) *Biophys. Struct. Mech. 9*, 181–191.
Bothner-By, A. A., Stephens, R. L., Lee, J., Warren, C. D., & Jeanloz, R. W. (1984) *J. Am. Chem. Soc. 106*, 811–813.
Brumfeld, V., & Miller, I. R. (1990) *Biochim. Biophys. Acta 1024*, 49–53.
Cafiso, D. S. (1994) *Annu. Rev. Biophys. Biomol. Struct.* (in press).
Chandrasekhar, K., Das, M. K., Kumar, A., & Balaram, P. (1988) *Int. J. Pept. Protein Res. 32*, 167–174.
Crippen, G., & Havel, T. (1978) *Acta Crystallogr. A34*, 282–284.
Duclohier, H., Molle, G., Dugast, J. Y., & Spach, G. (1992) *Biophys. J. 63*, 868–873.
Esposito, G., Carver, J. A., Boyd, J., & Campbell, I. D. (1987) *Biochemistry 26*, 1043–1050.
Esposito, G., Lesk, A. M., Molinari, H., Motta, A., Niccolai, N., & Pastore, A. (1992) *J. Mol. Biol. 224*, 659–670.
Fox, R. O., & Richards, F. M. (1982) *Nature 300*, 257–260.
Galaktionov, S. G., & Marshall, G. R. (1993) *Biophys. J. 65*, 608–617.
Gippert, G. P., Yip, P. F., Wright, P. E., & Case, D. A. (1990) *Biochem. Pharmacol. 40*, 15–22.
Griesinger, C., Otting, G., Wüthrich, K., & Ernst, R. R. (1988) *J. Am. Chem. Soc. 110*, 7870–7872.
Hall, J. E., Vodyanoy, I., Balasubramanian, T. M., & Marshall, G. R. (1984) *Biophys. J. 45*, 233–247.
Havel, T. F. (1990) *Biopolymers 29*, 1565–1585.
Havel, T. F., & Wüthrich, K. (1985) *J. Mol. Biol. 182*, 281–294.
Henry, G. D., & Sykes, B. D. (1990) *Biochemistry 29*, 6303–6313 .
Jeener, J., Meier, B. H., Bachmann, P., & Ernst, R. R. (1979) *J. Chem. Phys. 71*, 4546–4553.
Karle, I. L., & Balaram, P. (1990) *Biochemistry 29*, 6747–6756.
Karplus, M. (1959) *J. Chem. Phys. 30*, 11–15.
Kelsh, L. P., Ellena, J. E., & Cafiso, D. S. (1992) *Biochemistry 31*, 5136–5144.
Kumar, A., Ernst, R. R., & Wüthrich, K. (1980) *Biochem. Biophys. Res. Commun. 95*, 1–6.
Lehrer, R. I., Lichtenstein, A. K., & Ganz, T. (1993) *Annu. Rev. Immunol. 11*, 105–128.
Macura, S., & Ernst, R. R. (1980) *Mol. Phys. 41*, 95–117.
Nilges, M., Clore, G. M., & Gronenborn, A. M. (1988) *FEBS Lett. 229*, 317–24.
O'Neil, J. D. J., & Sykes, B. D. (1988) *Biochemistry 27*, 2753–2762.
Pardi, A., Billeter, M., & Wüthrich, K. (1984) *J. Mol. Biol. 180*, 741–751.
Piantini, U., Sorensen, O. W., & Ernst, R. R. (1982) *J. Am. Chem. Soc. 104*, 6800–6801.
Rance, M. (1987) *J. Magn. Reson. 74*, 557–564.
Rance, M., Sorensen, O. W., Bodenhausen, G., Wagner, G., Ernst, R. R., & Wüthrich, K. (1983) *Biochem. Biophys. Res. Commun. 117*, 479–485.
Sansom, M. S. P. (1993) *Eur. Biophys J. 22*, 105–124.
Williams, K. A., & Dever, C. M. (1991) *Biochemistry 30*, 8919–8923.
Wishart, D. S., Sykes, B. D., & Richards, F. M. (1992) *Biochemistry 31*, 1647–1651.
Wüthrich, K. (1986) *NMR of Proteins and Nucleic Acids*, pp 162–166, John Wiley & Sons, New York.
Yee, A. A., & O'Neil, J. D. J. (1992) *Biochemistry 31*, 3135–43.
Zasloff, M. (1987) *Proc. Natl. Acad. Sci. U.S.A. 84*, 5449–5453.